Int. J. Morphol.,
40(3):683-687, 2022.

The Morphological Challenge in Determining Nuclear Size and Shape in Anatomopathological Neoplasia Analysis

El Desafío Morfológico en la Determinación del Tamaño y Forma Nuclear en el Análisis Anatomopatológico de Neoplasias

Carlos Alberto Mandarim-de-Lacerda

MANDARIM-DE-LACERDA, C. A. The morphological challenge in determining nuclear size and shape in anatomopathological neoplasia analysis. *Int. J. Morphol., 40(3)*:683-687, 2022.

SUMMARY: From 1984 stereology was added to unbiased methods and procedures, i.e., counts became more reliable studying morphological images in a random and uniform isotropic way. Therefore, the orientation and sectioning methods adapted to stereological quantification are essential. A critical quantitative subject in practical pathology concerns diagnosing and classifying neoplasias. Pathologists evaluated different types of tumors by determining the nuclear roundness factor (NRF). NRF is calculated by the ratio between the nuclear radius obtained from the area and the perimeter. However, NRF is biased data because it depends on the sectioning orientation, nuclei shape, and section thickness. The stereology proposed an unbiased alternative to assess the nucleus from tumor cells, counteracting NRF quantitatively. Therefore, the volume-weighted mean nuclear volume has been used to prognostic tumors in several organs. In urology, this was used, for example, to study primary carcinoma of the bladder, renal and prostatic carcinomas.

KEY WORDS: Stereology; Morphometry; Tumor; Nucleus; Pathology.

INTRODUCTION

Pathologists have evaluated different types of tumors by determining the nuclear roundness factor (NRF) (Diamond *et al*., 1982; Mohler *et al*., 1988a,b), as the prostate cancer (Epstein *et al*., 1984; Shaeffer *et al*., 1992), and other types of neoplasia (Binder *et al*., 1998; Simeonov & Simeonova, 2006; Meachem *et al*., 2012).

The methodology needs measurement of the nuclear area and perimeter. The NRF can be assessed by the ratio of nuclear area and perimeter or, practically, by the ratio between the average diameter (or radius) calculated across the area and perimeter.

There are different ways to assess the area and diameter of nuclei, including image analysis (Mandarim-de-Lacerda *et al*., 2010). However, this text will use a classical test system for the data acquisitions.

Ewald Weibel and collaborators have proposed a test system that was at the time innovative, the M42, a frame composed of points and intersections, which includes 21 short lines (d) with test points at each end (d was designed in three staggered columns and seven equidistant lines, completing 42 test points) (Weibel *et al*., 1966; Weibel, 1979) (Fig. 1). Therefore, the test line length is calculated as 21d. Furthermore, an update of the former M42 test system was indicated by considering two consecutive frame boundaries as "forbidden lines," avoiding overestimating counts (Gundersen, 1977).

Further details on the construction and design of the M42 test system are illustrated in Figure 1 and corresponding literature (Weibel *et al*., 1966; Mandarim-de-Lacerda, 2003; Mandarim-de-Lacerda & del Sol, 2017). The nuclei hitting the exclusion lines should not be considered. Thus, points (circles at d extremities) and intersections (arrowheads) might be counted.

Laboratory of Morphometry, Metabolism, and Cardiovascular Diseases, Biomedical Center, Institute of Biology, The University of the State of Rio de Janeiro, Rio de Janeiro, Brazil.

FUNDING. The author is supported by the Conselho Nacional de Desenvolvimento Científico e Tecnológico (Brazil) (CNPq, Grant No 302.920/2016-1 and 40.60.81/2018-2), and Fundação Carlos Chagas Filho de Amparo à Pesquisa do Estado do Rio de Janeiro (Faperj, Grant No E-26/010.001274/2016, E-26/010.100947/2018, and E-26/200.936/2021). These foundations had no interference in the accomplishment and submission of the study.

Received: 2022-03-16 Accepted:2022-04-14

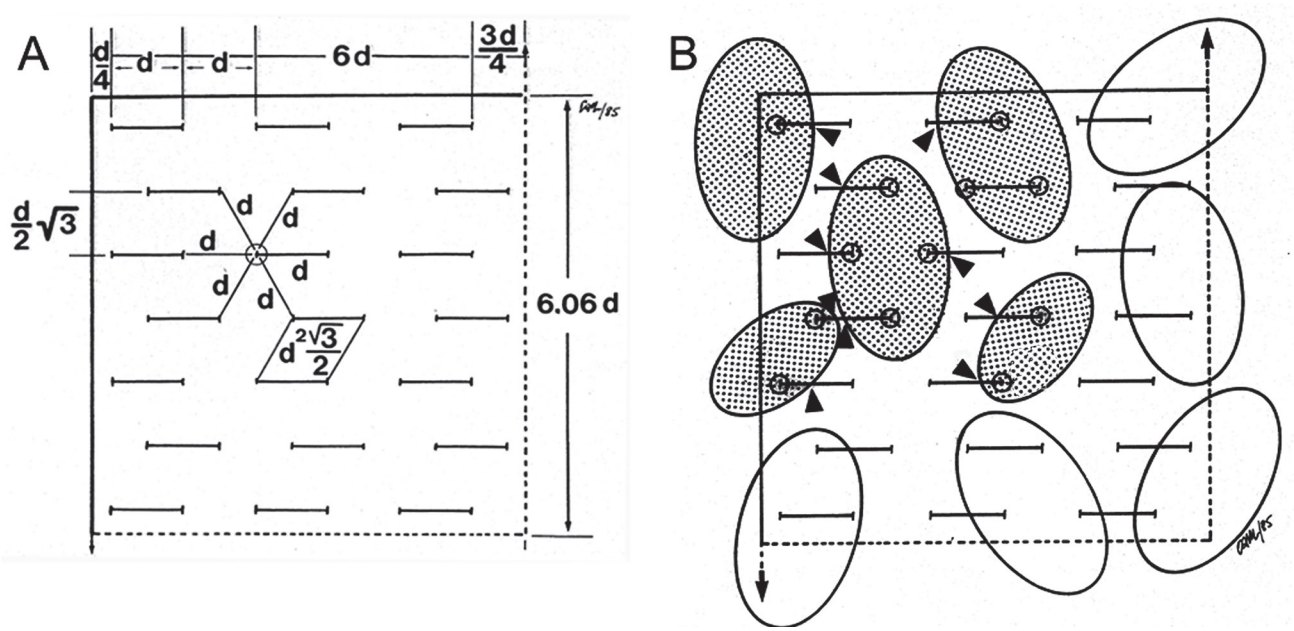

Fig. 1. The classical M42 test system. (A) construction plan; (B) diagram showing how to count points (open circles at the short line ends) and intersections (arrowheads).

1. Determination of the nuclear profile area (A_N):

$$A_N = \frac{P_p . A_p}{N_A} \qquad \mu m^2 \qquad (1)$$

Where P_p is the number of points hitting the nuclei, Ap is the area of each point predefined as $d^2 \sqrt{\frac{3}{2}}$ and N_A is the number of nuclei in the known frame area.

2. Determination of the nuclear radius calculated by A_N (R_A):

$$R_A = \sqrt{\frac{A_N}{\pi}} \qquad \mu m \qquad (2)$$

3. Determination of the nuclear perimeter (P_N):

$$P_N = \frac{A_T}{N_A} . \frac{\pi}{2} . \frac{I_N}{L_T} \qquad \mu m \qquad (3)$$

A_T is the test area equivalent to $36.37d^2$, I_N represents the intersections of the test line and nuclei, and L_T is the length of the test line (calculated as 21d).

4. Determination of the nuclear radius calculated by P_N (R_P):

$$R_P = \frac{P_N}{2.\pi} \qquad \mu m \qquad (4)$$

5. **Determination of the nuclear roundness factor (NRF)**

$$NRF = \frac{R_P}{R_A} \qquad \mu m^o \qquad (5)$$

The NRF must be close to unity when the cell nucleus is approximately spherical. NRF values that deviate from unity indicate non-spherical nuclear shapes. Bizarre nuclear forms are present in neoplasia and are more bizarre the more undifferentiated the tumors are (De Benedictis *et al*., 1992; Wählby *et al*., 2004; Nafe *et al*., 2005). Therefore, pathologists might use NRF determination as additional data in diagnosing tumors.

However, the nuclear profile depends on the section orientation and thickness. The equatorial section of the nucleus compared to the polar section will estimate different sizes of the same nucleus besides the nucleus might be spherical, elliptical, or random bizarrely (Mandarim-de-Lacerda & del Sol, 2017). In addition, the cut orientation might add additional bias to the analysis (the leading cause of these biases is the orientation of sectioning and the not perfectly

spherical nuclear form). Also, a thick section might produce additional bias correlating to small and prominent nuclei (Gundersen *et al*., 1983; Andersen & Gundersen, 1999). So, nuclear measurement can be nonreproducible, thus, a problem.

The "volume-weighted mean nuclear volume" (MNV) was recommended as an unbiased alternative to evaluate the tumor nuclei instead of the NRF (Gundersen & Jensen, 1985; Gundersen, 1986; Sørensen, 1992). The rationale for using MNV is that the calculation of NRF usually does not give an accurate measure of cell nuclei. So, the analyses generally spent much time using microscopic calipers or image analysis systems without the certainty of nuclear measurement accuracy.

Using a logarithmic scale l_o^3 built of 15 classes is proposed to overcome the challenges imposed by the nuclear shape (Fig. 2). Then, nuclei are measured using the ranges in classes (Gundersen & Jensen, 1985).

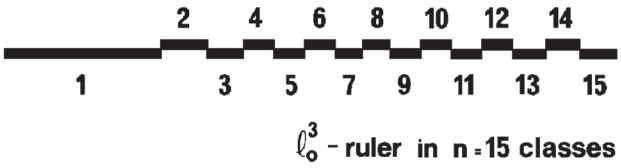

Fig. 2. Logarithmic ruler. Fifteen logarithmic classes ruler was proposed to measure the nucleus profile length in sampled nuclei (see Fig. 4) (details in Sørensen, 1991).

Which and how many nuclei to measure? This question is answered by sampling the nuclei in a targeted test area (randomly). It was advised that at least 50 nuclei per group should be counted to obtain satisfactory MNV results (Gundersen & Jensen, 1985).

In this method, the test area shows marks on the upper and right sides [construction details are provided in the reference (Sørensen, 1991)], which help align a test system with points (possibly built using a transparent sheet to be applied over the test area), or other more recent computerized option (Fig. 3).

The spacing between the rows and between the points should not be less than the average size of the nuclei. The system must be aligned through the test area marks and the x and y axes cross (bottom left).

The steps for data acquisition might be summarized as follows:

a) First, the test system should be aligned with the test area, starting with a random number among the mark numbers (defined by lottery). Next, the procedure should be repeated in each new image to obtain new options for the alignment of the test system.

b) Sampled nuclei should be measured with the 15 classes logarithmic l_o^3 ruler (Fig. 2) over the line of the test system, the path on the nucleus (in bold in Fig. 4).

c) Although it is not necessary to transform the measures taken classes with the l_o^3 ruler at values expressed in μm^3, we can proceed as indicated below to make this transformation (Sorensen, 1991):

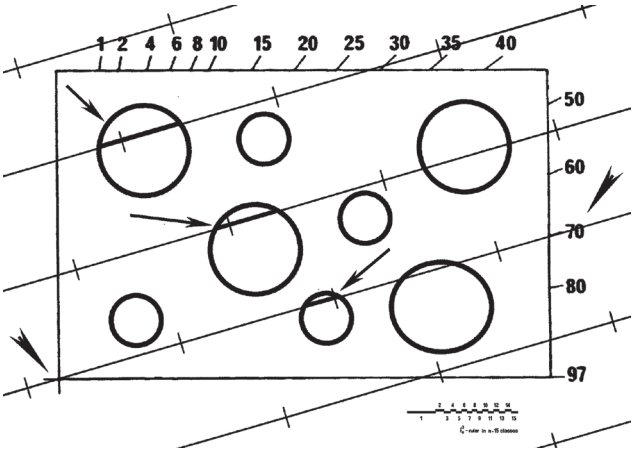

Fig. 4. Volume-weighted mean nuclear volume estimation diagram. The nuclei (circles) within a test area are sampled by hitting the test points (arrows) and then measured (bold line segments) with the fifteen logarithmic classes ruler. The test system was aligned (between # 70 and the x and y cross, arrowheads). Three nuclei profiles were sampled in the example, and nuclear length over the test line was measured (in bold).

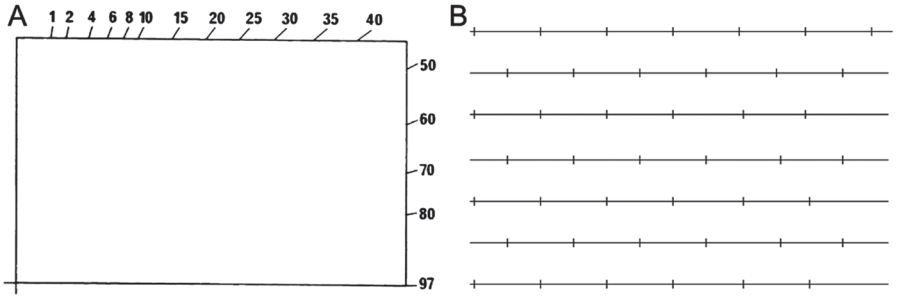

Fig. 3. Test area and test system for volume-weighted mean nuclear volume estimation. (A) Test area construction plan adding alignment marks; (B) Test system with lines and points (modified from Sørensen, 1991).

6. Volume-weighted mean nuclear volume

$$MNV = \frac{\pi}{3} \cdot \frac{\sum l_0^3}{P_N} \cdot \left(\frac{L_n \cdot 1000}{300.M} \right) \quad \mu m^3, \quad (6)$$

P_N is the nuclei sampled, Ln is the ruler's length in millimeters, and M is the final magnification.

The calculations can be done in a spreadsheet (like Excel), as shown in Figure 5. The counts of logarithmic ruler classes sampled in the images are put on the spreadsheet's upper side. The example shows research with four research groups (e.g., control, treatment 1, treatment 3, and treatment 3). In addition, formula 6 can be adapted for MNV determination using the spreadsheet data acquisition (the spreadsheet's lower side shows calculation). Then:

$$MNV = \frac{\pi}{3} \cdot \frac{\sum (E.F)}{\sum F} \cdot \left(\frac{10^4}{M} \right) \quad \mu m^3, \quad (7)$$

In conclusion, performing the MNV quantification in the pathologist's daily practice is not simple. Hence, after years of the method description, few published studies on MNV are found in Pubmed (less than 100 articles in March 2022). However, to advance knowledge and scientific research, the method may have greater applicability and be used for dubious cases or to advance the characterization of a type of neoplasia, like the prostate cancer correlation with the Gleason grade (Leze *et al*., 2014).

Groups	Class 1	Class 2	Class 3	Class 4	Class 5	Class 6	Class 7	Class 8	Class 9	Class 10	Class 11	Class 12	Class 13	Class 14	Class 15
1	34	98	108	83	43	13	15	10	6	0	0	0	0	0	0
1	13	32	59	99	79	83	46	26	12	4	2	0	0	0	0
1	7	50	76	116	104	68	39	13	7	1	0	0	0	0	0
1	12	25	52	66	83	78	74	35	13	7	4	2	1	0	0
1	64	131	115	62	35	70	32	25	6	0	0	0	0	0	0
2	13	31	58	65	53	37	23	19	8	5	2	0	0	0	0
2	15	71	90	112	82	43	17	15	3	2	0	0	0	0	0
2	8	27	50	58	36	49	27	15	11	5	0	0	0	0	0
2	11	50	75	102	75	50	26	14	5	3	2	0	0	0	0
2	7	33	68	90	101	104	56	38	4	5	4	2	0	0	0
3	1	8	22	46	55	45	63	50	42	50	13	15	7	10	5
3	0	6	13	19	33	64	61	69	59	65	39	29	16	14	11
3	2	1	12	22	42	42	46	56	46	39	32	37	12	10	5
3	0	2	26	43	50	70	46	57	48	55	38	21	14	5	4
3	0	3	10	20	35	62	72	86	102	92	36	38	23	10	3
Control	34	67	97	92	91	58	7	4	0	0	0	0	0	0	0
Control	28	65	89	80	49	22	5	3	0	0	0	0	0	0	0
Control	32	96	85	63	37	10	9	1	1	0	0	0	0	0	0
Control	59	100	105	47	19	15	1	0	0	0	0	0	0	0	0
Control	52	86	88	84	26	10	2	0	0	0	0	0	0	0	0

		Group 1			Group 2			Group 3			Group 4		
Class	E	F	G	H	F	G	H	F	G	H	F	G	H
	(mm)	(median)	E^4F (mm^3)	$E^2.F$ (mm^b)	(median)	E^4F (mm^3)	$E^2.F$ (mm^b)	(median)	E^4F (mm^3)	$E^2.F$ (mm^b)	(median)	E^4F (mm^3)	$E^2.F$ (mm^b)
1	0,22	13,00	2,86	0,63	11,00	2,42	0,53	0,00	0,00	0,00	34,00	7,48	1,65
2	0,71	50,00	35,50	25,21	33,00	23,43	16,64	3,00	2,13	1,51	86,00	61,06	43,35
3	1,29	76,00	98,04	126,47	68,00	87,72	113,16	13,00	16,77	21,63	89,00	114,81	148,10
4	1,96	83,00	162,68	318,85	90,00	176,40	345,74	22,00	43,12	84,52	80,00	156,80	307,33
5	2,76	79,00	218,04	601,79	75,00	207,00	571,32	42,00	115,92	319,94	37,00	102,12	281,85
6	3,70	70,00	259,00	958,30	49,00	181,30	670,81	62,00	229,40	848,78	15,00	55,50	205,35
7	4,81	39,00	187,59	902,31	26,00	125,06	601,54	61,00	293,41	1411,30	5,00	24,05	115,68
8	6,12	25,00	153,00	936,36	15,00	91,80	561,82	57,00	348,84	2134,90	1,00	6,12	37,45
9	7,66	7,00	53,62	410,73	5,00	38,30	293,38	48,00	367,68	2816,43	0,00	0,00	0,00
10	9,48	1,00	9,48	89,87	5,00	47,40	449,35	55,00	521,40	4942,87	0,00	0,00	0,00
11	11,62	0,00	0,00	0,00	2,00	23,24	270,05	36,00	418,32	4860,88	0,00	0,00	0,00
12	14,14	0,00	0,00	0,00	0,00	0,00	0,00	29,00	410,06	5798,25	0,00	0,00	0,00
13	17,12	0,00	0,00	0,00	0,00	0,00	0,00	14,00	239,68	4103,32	0,00	0,00	0,00
14	20,63	0,00	0,00	0,00	0,00	0,00	0,00	10,00	206,30	4255,97	0,00	0,00	0,00
15	24,76	0,00	0,00	0,00	0,00	0,00	0,00	5,00	123,80	3065,29	0,00	0,00	0,00
	Sum	443,00	1179,81	4370,52	379,00	1004,07	3894,33	457,00	3336,83	34665,59	347,00	527,94	1140,77
Magnification M =	2200,0	**Group 1**	**n = 5**		**Group 2**	**n = 5**		**Group 3**	**n = 5**		**Group 4**	**n = 5**	
	$v_{V=}$	**262,62**	**µm³**		**261,24**	**µm³**		**720,01**	**µm³**		**150,03**	**µm³**	
	CE =	**0,030**	**3,0%**		**0,035**	**3,5%**		**0,030**	**3,0%**		**0,035**	**3,5%**	
	CV =	**0,625**	**62,5%**		**0,681**	**68,1%**		**0,650**	**65,0%**		**0,648**	**64,8%**	
	SD =	**164,2**	**µm³**		**178,0**	**µm³**		**468,2**	**µm³**		**97,3**	**µm³**	

Fig. 5. Spreadsheet (Excel) estimates the MNV based on counts and measurements. When hitting test points, nuclei are sampled in the test area (Fig. 4). The nuclear profile length is measured over the test line (whose orientation will change randomly with each new image). The counts and measurements are shown in the spreadsheet's upper portion, transformation in the metric system, and statistics in the spreadsheet's lower portion.

MANDARIM-DE-LACERDA, C. A. El desafío morfológico en la determinación del tamaño y forma nuclear en el análisis anatomopatológico de neoplasias. *Int. J. Morphol., 40(3)*:683-687, 2022.

RESUMEN: A partir de 1984 se agregó la estereología a los métodos y procedimientos sin distorción, es decir, los conteos se volvieron más confiables al estudiar imágenes morfológicas de forma aleatoria e isotrópica uniforme. Por tanto, los métodos de orientación y seccionamiento adaptados a la cuantificación estereológica son fundamentales. Un tema cuantitativo crítico en la patología práctica se refiere al diagnóstico y clasificación de las neoplasias. Los patólogos evaluaron diferentes tipos de tumores determinando el factor de redondez nuclear (NRF). NRF se calcula por la relación entre el radio nuclear obtenido del área y el perímetro. Sin embargo, NRF son datos distorsionados debido a que dependen de la orientación de la sección, la forma de los núcleos y el grosor de la sección. La estereología propuso una alternativa imparcial para evaluar el núcleo de las células tumorales, contrarrestando cuantitativamente el NRF. Por lo tanto, el volumen nuclear medio ponderado se ha utilizado para pronosticar tumores en varios órganos. En urología, esto se utilizó, por ejemplo, para estudiar el carcinoma primario de vejiga, carcinomas renales y prostáticos.

PALABRAS CLAVE: Estereología; Morfometría; Tumor; Núcleo; Patología.

REFERENCES

Andersen, B. B. & Gundersen, H. J. Pronounced loss of cell nuclei and anisotropic deformation of thick sections. *J. Microsc., 196(Pt. 1)*:69-73, 1999.

Binder, M.; Steiner, A.; Mossbacher, U.; Hunegnaw, M.; Pehamberger, H. & Wolff, K. Estimation of the volume-weighted mean nuclear volume discriminates keratoacanthoma from squamous cell carcinoma. *Am. J. Dermatopathol., 20(5)*:453-8, 1998.

De Benedictis, G.; Ricco, R.; Lettini, T.; Serio, G.; Pennella, A.; Troia, M.; Napoli, A. & Pesce Delfino, V. Morphometrical investigation of medulloblastoma nuclei by S.A.M. (Shape Analytical Morphometry) software system. *Pathol. Res. Pract., 188(4-5)*:576-80, 1992.

Diamond, D. A.; Berry, S. J.; Jewett, H. J.; Eggleston, J. C. & Coffey, D. S. A new method to assess metastatic potential of human prostate cancer: relative nuclear roundness. *J. Urol., 128(4)*:729-34, 1982.

Epstein, J. I.; Berry, S. J. & Eggleston, J. C. Nuclear roundness factor. A predictor of progression in untreated Stage A2 prostate cancer. *Cancer, 54(8)*:1666-71, 1984.

Gundersen, H. J. & Jensen, E. B. Stereological estimation of the volume-weighted mean volume of arbitrary particles observed on random sections. *J. Microsc., 138(Pt. 2)*:127-42, 1985.

Gundersen, H. J. G. Notes on the estimation of the numerical density of arbitrary profiles: the edge effect. *J. Microsc., 111(2)*:219-23, 1977.

Gundersen, H. J. G.; Andersen, B. S. & Fløe, H. Estimation of section thickness unbiased by cutting-deformation. *J. Microsc., 131(1)*:RP3-RP4, 1983.

Gundersen, H. J. Stereology of arbitrary particles. A review of unbiased number and size estimators and the presentation of some new ones, in memory of William R. Thompson. *J. Microsc., 143(Pt. 1)*:3-45, 1986.

Leze, E.; Maciel-Osorio, C. F. E. & Mandarim-de-Lacerda, C. A. Advantages of evaluating mean nuclear volume as an adjunct parameter in prostate cancer. *PLoS One, 9(7)*:e102156, 2014.

Mandarim-de-Lacerda, C. A. & del Sol, M. Tips for Studies with Quantitative Morphology (Morphometry and Stereology). *Int. J. Morphol., 35(4)*:1482-94, 2017.

Mandarim-de-Lacerda, C. A. Stereological tools in biomedical research. *An. Acad. Bras. Cienc., 75(4)*:469-86, 2003.

Mandarim-de-Lacerda, C. A.; Fernandes-Santos, C. & Aguila, M. B. Image analysis and quantitative morphology. *Methods Mol. Biol., 611*:211-25, 2010.

Meachem, M. D.; Burgess, H. J.; Davies, J. L. & Kidney, B. A. Utility of nuclear morphometry in the cytologic evaluation of canine cutaneous soft tissue sarcomas. *J. Vet. Diagn. Invest., 24(3)*:525-30, 2012.

Mohler, J. L.; Partin, A. W.; Epstein, J. I.; Lohr, W. D. & Coffey, D. S. Nuclear roundness factor measurement for assessment of prognosis of patients with prostatic carcinoma. II. Standardization of methodology for histologic sections. *J. Urol., 139(5)*:1085-90, 1988a.

Mohler, J. L.; Partin, A. W.; Lohr, W. D. & Coffey, D. S. Nuclear roundness factor measurement for assessment of prognosis of patients with prostatic carcinoma. I. Testing of a digitization system. *J. Urol., 139(5)*:1080-4, 1988b.

Nafe, R.; Schlote, W. & Schneider, B. Histomorphometry of tumour cell nuclei in astrocytomas using shape analysis, densitometry and topometric analysis. *Neuropathol. Appl. Neurobiol., 31(1)*:34-44, 2005.

Shaeffer, J.; Tegeler, J. A.; Kuban, D. A.; Philput, C. B. & el-Mahdi, A. M. Nuclear roundness factor and local failure from definitive radiation therapy for prostatic carcinoma. *Int. J. Radiat. Oncol. Biol. Phys., 24(3)*:431-4, 1992.

Simeonov, R. & Simeonova, G. Computerized morphometry of mean nuclear diameter and nuclear roundness in canine mammary gland tumors on cytologic smears. *Vet. Clin. Pathol., 35(1)*:88-90, 2006.

Sørensen, F. B. Quantitative analysis of nuclear size for objective malignancy grading: a review with emphasis on new, unbiased stereologic methods. *Lab. Invest., 66(1)*:4-23, 1992.

Sørensen, F. B. Stereological estimation of the mean and variance of nuclear volume from vertical sections. *J. Microsc., 162(2)*:203-29, 1991.

Wählby, C.; Sintorn, I. M.; Erlandsson, F.; Borgefors, G. & Bengtsson, E. Combining intensity, edge and shape information for 2D and 3D segmentation of cell nuclei in tissue sections. *J. Microsc., 215(1)*:67-76, 2004.

Weibel, E. R. 1979. *Stereological Methods. Practical Methods for Biological Morphometry.* Toronto, Academic Press, 1979.

Weibel, E. R.; Kistler, G. S. & Scherle, W. F. Practical stereological methods for morphometric cytology. *J. Cell Biol., 30(1)*:23-38, 1966.

Corresponding author:
Carlos Alberto Mandarim-de-Lacerda
Centro Biomedico, Instituto de Biologia
Universidade do Estado do Rio de Janeiro
Av 28 de Setembro 87 fds
20551-030 Rio de Janeiro
BRAZIL

E-mail: mandarim@uerj.br
mandarim.ca@gmail.com

Website: http://www.lmmc.uerj.br